On the Trade-Off between Battery Size and Sustainability for a Fuel Cell Hybrid Electric Vehicle

(article starts on next page)

On the Trade-Off between Battery Size and Sustainability for a Fuel Cell Hybrid Electric Vehicle

Tatiana Santos Andrade,* Shangwei Zhou, Jia Di Yang, Rhodri Jervis, and Torbjörn Thiringer

Fuel cell vehicles (FCVs) offer a promising route to decarbonization of the transport sector. Since all FCVs benefit from hybridization with a small battery pack, understanding the impact and limitations of the fuel cell and battery sizing regarding the vehicle's energy efficiency and environmental aspects is needed to support the development of these technologies. Herein, fuel cell hybrid vehicles with different battery sizes concerning the impact on energy efficiency and carbon emissions for three different drive cycles are investigated. Results suggest that increasing the battery capacity (up to 5 kWh) can considerably lower the hydrogen consumption. The fuel consumption saving can balance the carbon emissions for the extra battery size, up to 50 000 km driven, if gray hydrogen is used as a fuel. In the case of green hydrogen fuel, the extra battery size is mostly justified only if speed-aggressive driving is frequently used and/or if the green hydrogen production generates close to 5 kg-CO_2/kg-H_2.

1. Introduction

As an urgent response to the environmental issues caused by fossil fuel-based vehicles, the transportation sector is experiencing a rapidly growing electrification.[1–3] Among zero tailpipe carbon emission vehicles, battery and fuel cell electric cars have emerged as the most promising options. Despite their exponential commercialization in the last decade, some challenges still restrain market penetration.[4–7] Regarding fuel cell vehicles (FCVs), besides the uncertainty of the hydrogen economy,[8,9] improving car efficiency and evaluating its sustainability have arisen as major concerns toward their development.[10–15]

T. S. Andrade, T. Thiringer
Department of Electrical Engineering
Chalmers University of Technology
41296 Gothenburg, Sweden
E-mail: tatianas@chalmers.se

S. Zhou, J. D. Yang, R. Jervis
Electrochemical Innovation Lab
Department of Chemical Engineering
University College London
London WC1E 7JE, UK

The ORCID identification number(s) for the author(s) of this article can be found under https://doi.org/10.1002/ente.202402411.

FCVs are hybrid vehicles, since their powertrain is also composed of a battery to support the power dynamics; this battery is usually significantly smaller, about 50 times lower capacity, than a battery electric vehicle pack. Being only fueled by hydrogen, balancing the battery charging/discharging operation is challenging, while minimizing fuel cell consumption.[14–18] For instance, increasing the battery capacity can improve vehicle efficiency by allowing more buffer energy in the system; however, it is limited by the battery's added extra weight and the fuel cell efficiency profile.[18] The rule-based energy management strategy established as the most applicable in real vehicle applications,[15] was linked to battery sizing by Hu et al.[19] The study proposes that power demand-based and state-of-charge (SOC)-based control were more suitable for a powertrain composed of large and small batteries (<5 kWh), respectively. Despite the study's limitation to a certain drive cycle, that is, the new European driving cycle, and downsized fuel cell, that is, compared to a commercial FCV, it has been shown that small batteries are more sensitive to the vehicle power load. However, smaller batteries, besides being lighter, present a lower carbon print in their manufacturing process. Thus, defining the control strategy and the battery size becomes a trade-off with sustainability that, to the best of our knowledge, is mostly neglected in current evaluations. Even though FCVs have no tailpipe emissions, depending on the hydrogen source, that is, gas reforming, gas reforming with carbon capture, and renewables (gray, blue, and green hydrogen, respectively), the fuel consumption and battery size can be more or less relevant.[20,21]

Therefore, in this work, we aim to investigate the combined impact of battery sizing and control strategy on the efficiency of FCVs across different drive cycles. Unlike existing studies, which typically address these aspects separately, we also address the trade-off of battery sizing and carbon emissions. The specific contributions of this work are: 1) modeling an FCV powertrain based on collected data of a commercial FCV and simulation for the Worldwide Harmonized Light Vehicles Test Procedure (WLTP), NREL2VAIL, and US06 drive cycles. 2) Quantifying and analyzing hydrogen consumption in the designed FCV using a varied battery capacities and control strategies, that is, SOC- and power demand-based, based on collected data from a commercial FCV. 3) Analyzing whether the energy-consumption

ADVANCED
SCIENCE NEWS
www.advancedsciencenews.com

Energy Technology
Generation, Conversion, Storage, Distribution
www.entechnol.de

reduction provided by a bigger battery also reduced carbon emissions, considering the FCV fueled by gray, blue, or green hydrogen.

2. Methodology

2.1. Vehicle Modeling

To design and model the vehicle system diagram, the following components were considered: the vehicle dynamics (the wheels), gear, electric motor, inverter, battery, converter, and the fuel cell. All the components were modeled in a steady-state using MATLAB. The vehicle powertrain is represented in **Figure 1** and further described.

The vehicle dynamics, that is, concerning the total force acting on the wheels, was assumed to be the sum of the friction, rolling, grading, and acceleration forces.[22]

$$F_{\text{wheels}} = F_{\text{friction}} + F_{\text{rolling}} + F_{\text{grading}} + F_{\text{acc}} \tag{1}$$

in which

$$F_{\text{friction}} = \frac{1}{2}\rho_\alpha C_d A_f v_{\text{car}}^2 \tag{2}$$

$$F_{\text{rolling}} = C_r m g \tag{3}$$

$$F_{\text{grading}} = C_r m g \cos(\alpha) \tag{4}$$
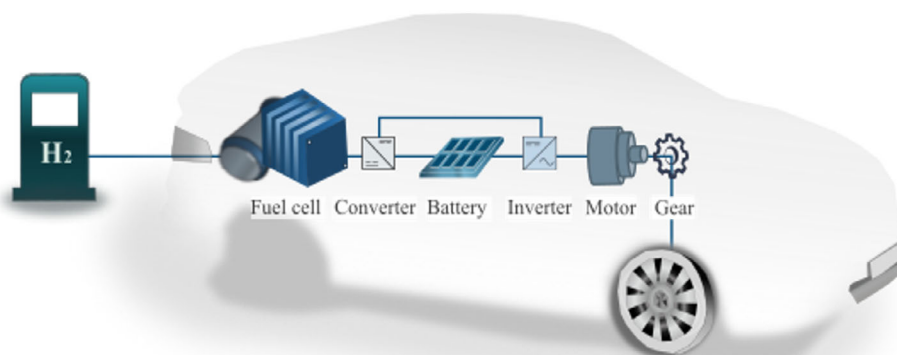
$$F_{\text{acc}} = m a_{cc} \tag{5}$$

where ρ_α refers to the air density, C_d is the aerodynamic drag coefficient, A_f is the vehicle's cross-sectional area, v_{car} is the vehicle speed, C_r is the rolling resistance coefficient, m is the vehicle's mass, g is the gravity constant, α is the road inclination angle, and a_{cc} is the acceleration. The vehicle specifications are listed in **Table 1**.

The powertrain components, shown in Figure 1, were modeled based on experimental data previously reported. For instance, the single-speed gear with 97% efficiency and a ratio of 10 was assumed.[23] The electric motor was an eight-pole permanent magnet synchronous motor and the inverter was DC–AC
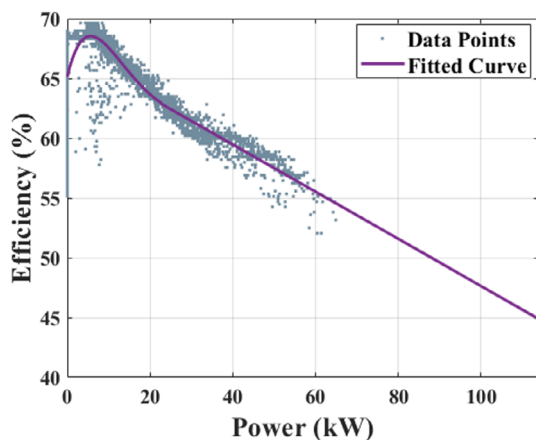
Table 1. Vehicle specifications.

Parameter [initials]	Value [unit]
Mass [m] - FCV	1990 + Battery mass [kg]
Air density [ρ_α]	1.225 [kg m^{-3}]
Aerodynamic drag coefficient [C_d]	0.3 [–]
Cross-sectional area [A_f]	2.5 [m^2]
Rolling resistance coefficient [C_r]	0.01 [–]
Gravity constant [g]	9.82 [m s^{-2}]
Wheel radius [r]	0.3 [m]

insulated-gate bipolar transistor converter as previously described.[24,25] The converter between the fuel cell and the battery was assumed to have 95% efficiency based on refs. [26,27]. The battery model was based on reported data of a pouch-cell Li-ion battery used in electric vehicles with a nominal voltage of 3.6 V and a resistance of 3 mΩ per cell.[26,27] The battery size, that is, 9.2 kWh in the reference battery, was scaled to four different capacities: 1.6, 3.2, 4.8, and 6.4 kWh modeled in a 100-cell series composition. The smallest size corresponds to the battery size of a commercial FCV, that is, Toyota Mirai,[28] abbreviated in this work as the Std size. The battery weight was assumed to be 6.25 kg per kWh. The battery-maximum pulse C-rates were 10 and 20 C for charging and discharging, respectively, based on refs. [29,30]. Thus, the bigger the batteries, the higher the charging and discharging C-rates. All the simulations started with the battery at 80% SOC. The 114 kW maximum-power fuel cell was designed based on collected data from a 370-cell stack of a commercial FCV, that is, Toyota Mirai. The FCV was equipped with a controller area network data logger system that measures voltage and current flow signals of the battery, and the fuel cell as previously reported.[31] To fit the data points, the first part of the curve, power up to 20 kW, a six-degree polynomial profile was used, while for values higher than 20 kW up to 114 kW, a linear relation was established. The data collected along with the fitted curve used in the model are shown in **Figure 2**, showing a maximum efficiency of around 67% which aligns with the reported data.[28]

Figure 1. System diagram representation for the fuel cell vehicle powertrain.

**ADVANCED
SCIENCE NEWS**
www.advancedsciencenews.com

Energy Technology
Generation, Conversion, Storage, Distribution

www.entechnol.de

Figure 2. Fuel cell profile obtained from the commercial FCV and the fitted curve used in the model.

Two control strategies were implemented in the FCV to split the power between the fuel cell and the battery, that is, power and SOC-based. The implemented controls were based on the profile of collected data from the FCV previously reported,[31] with modifications as further described. Some common features were designed for both control strategies during low-load power, deceleration, and steady-state speed as per the previous description. Meanwhile, distinct modeling was implemented during the acceleration peaks aiming at investigating the control strategy's impact on vehicle energy consumption. Thus, in both strategies, the fuel cell avoids operation at a load lower than 5 kW with the battery providing most of the power. During deceleration, the battery takes the regenerative braking power. The fuel cell provides power at steady-state speed, that is, $a_{cc} = 0$, and most of the power during acceleration peaks. While the fuel cell is the power source during steady-state speed, both the fuel cell and the battery share the power during acceleration, that is, $a_{cc} > 0$. At the acceleration peaks, the power that comes from the fuel cell and the battery differs for each control strategy based on either the battery SOC or the power load. In the first strategy, a SOC-based control, the fuel cell power output ranged from 5 to 114 kW, linearly correlated with the battery SOC, which varied between 30% and 90%. In that case, the fuel cell balances the battery SOC by providing more power as the battery discharges. Thus, the lower the SOC, the higher the fuel cell, for example, 114 kW at 30% SOC. For the second strategy, a load-based control was implemented. In that case, the battery and the fuel cell share a percentage of the total load required from the power source in the acceleration peaks, that is, 20/80. Thus, in that case, the fuel cell is always the main power source during the acceleration supported by the battery.

The designed powertrain was simulated for the WLTP Class 3, US06, and NREL2VAIL drive cycles. The selected drive cycles have aimed at covering average driving conditions, and being representative of extreme conditions that would require a severe battery usage. The WLTP, which is representative of standard real driving conditions, is the current global standard drive cycle used to evaluate car emissions. This drive cycle is 23.25 km long, with an average speed of 46.5 km h^{-1}. While the WLTP

represents an average driving condition, the US06 and NREL2VAIL were used here to evaluate extreme driving conditions, that is, aggressive and uphill drive cycles. Thus, the US06 has high speeds with an average speed of 77 km h^{-1} and quick acceleration peaks for a 12.8 km long course. Meanwhile, the NREL2VAIL represents high-speed driving on a rocky mountain track in Colorado. **Figure 3**A–C shows the drive cycle profile of WLTP, US06, and NREL2VAIL. Figure 3D shows the elevation profile of NREL2VAIL. Both WLTP and US06 were implemented considering no road inclination.

2.2. Carbon Emission Analysis

To relate the carbon emissions of the vehicle fuel consumption and the battery size, the amount of km-driven to compensate for the extra carbon emission added by the battery's extra weight and its related manufacturing process were calculated. A range of 60 to 120 kg CO_2 emissions per kWh related to the battery manufacturing process was assumed considering reported values for lithium-ion batteries.[32] The amount of km-driven was calculated as the ratio of the battery's extra emissions and the vehicle's reduced consumption per km.

$$d_{\text{compensation}}(\text{km}) = \frac{\text{Battery extra emissions (kg)}}{\text{Fuel emissions}\left(\frac{\text{kg}}{\text{km}}\right)} \quad (6)$$

For the fuel consumption, the CO_2 emissions associated with hydrogen production from the different sources were assumed. The potential fuel sources for the vehicle were gray, blue, and green hydrogen, where gray hydrogen is related to the hydrogen produced by natural gas reforming, blue hydrogen is the gray hydrogen with carbon capture, and green hydrogen is hydrogen produced by renewables, for example, solar and wind energy. The CO_2 emissions per kg of hydrogen produced are estimated to be in range from 10 to 15 kg for gray hydrogen, 5 to 10 kg for blue hydrogen, and 0 to 5 kg for green hydrogen, with the
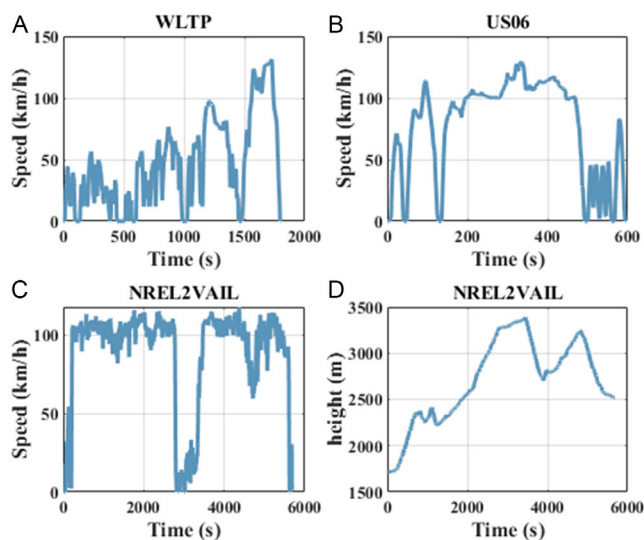
Figure 3. Speed profile for A) the WLTP Class 3, B) US06, C) NREL2VAIL drive cycles, and D) elevation profile for the NREL2VAIL drive cycle.

2402411 (3 of 6)

ADVANCED
SCIENCE NEWS
www.advancedsciencenews.com

Energy Technology
Generation, Conversion, Storage, Distribution
www.entechnol.de

variation in each range reflecting differences in production methods, energy sources, and technological efficiencies.[20,21]

3. Results and Discussion

The energy consumption per kilometer regarding the control strategies and the battery size has revealed varied trends according to the drive cycle, as shown in **Figure 4** and discussed.

As expected, the FCV was more energy-consuming, that is, about 50% higher, when driving in the NREL2VAIL and US06 cycles due to their grading and/or speed-aggressive profile. Other extreme driving conditions, such as intense cold weather, although beyond the scope of this work, have been reported to be beneficial for FCV efficiency due to the possibility of using heat from the system. Concerning the control strategy, the hydrogen consumption per kilometer was generally lower by using the load-based control for all the drive cycles considered, as shown

in Figure 4, demonstrating the advantage of this strategy compared to the SOC-based. Regarding the battery size, double-sizing the battery capacity was more suitable than the Std size for all the drive cycles analyzed, as shown by the lower hydrogen consumption per kilometer in Figure 4. However, the further increase was dependent on the control and drive cycle. Generally, bigger batteries provide more buffer energy in the system, allowing for low fuel consumption. However, the buffered energy supplied by the double-sized battery in the load-based control, already has sufficient capacity to minimize the losses caused by the battery restraints, that is, braking energy recovery limitation due to the maximum battery charging or the battery SOC limits. Thus, in the load-based control, bigger batteries (>3.2 kWh), except in the US06 drive cycle as further discussed, did not provide significant fuel savings to compensate for the increased weight of the battery, as shown in Figure 4. **Figure 5** displays the losses per component of the FCV composed of the single (Std) and double sized (2Std) batteries, showing the
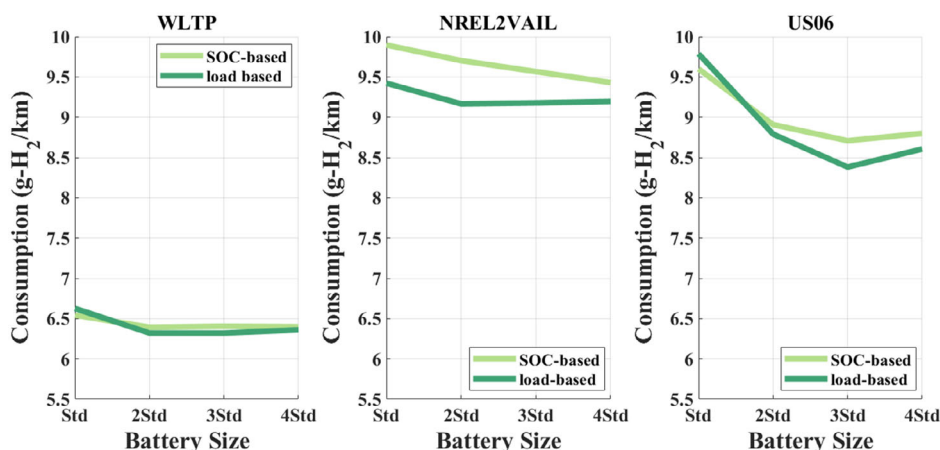
Figure 4. Hydrogen consumption per km (g-H_2 km^{-1}) for the FCV in the WLTP, NREL2VAIL, and US06 drive cycles comprising different battery capacities. "Std" stands for the capacity of those present in a commercial FCV, while "2Std", "3Std", and "4Std" represent a battery of 2, 3, and 4 times bigger. The consumption was evaluated for two control strategies: SOC-based, based on the battery SOC, and load-based, based on the load required from the drive cycle.
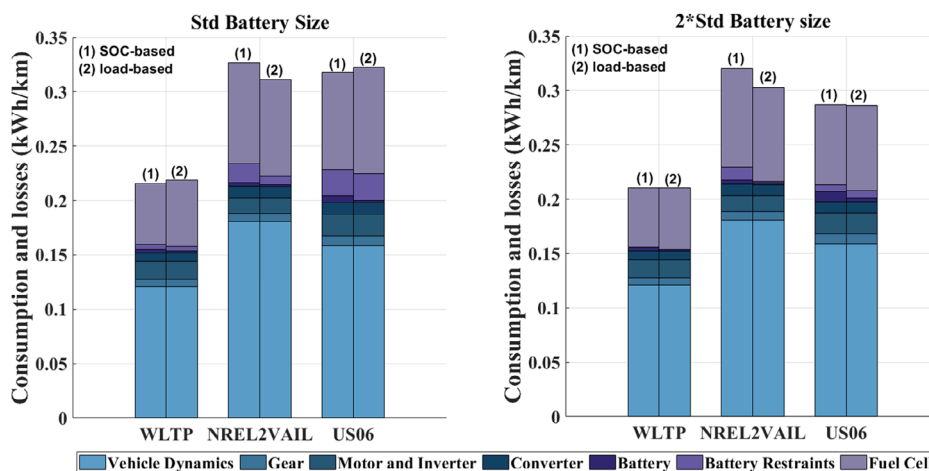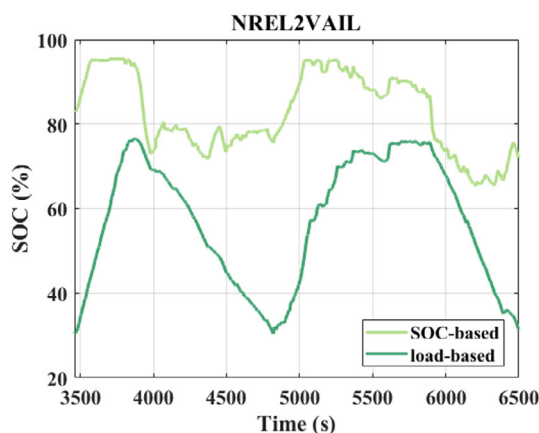

Figure 5. Consumption and losses per km for the FCV composed of the single size (Std) and double size (2*Std) battery capacity in the WLTP, NREL2VAIL, and US06 drive cycle.

significant reduction in the battery restrain losses, that is, related to the limitations in the maximum battery charging and SOC limit for the double-sized battery. The differences in the drive cycles and the control strategy are further discussed.

Up to the double-sized batteries, the control strategies did not show significant differences in the hydrogen consumption for the WLTP and the US06 drive cycles. In the SOC-based control, the fuel cell operation is shifted to higher efficiencies, adding fewer losses from the fuel cell. However, the battery operates at higher power, which is related to more electrical losses in this component; thus, balancing the overall vehicle fuel consumption, as shown in **Figure 6**. Despite the similar consumption for the WLTP and US06 using different controls, the SOC-based control was more efficiency-limiting in the NREL2VAIL compared to the load-based demonstrated by the higher overall consumption in Figure 5. In the SOC-based control, the fuel cell operation maintains the SOC level as soon as the battery discharges, not allowing enough battery capacity for the braking energy downhill in the NREL2VAIL. The load-based control reduces this issue, which enables the SOC fluctuation dependent on the drive cycle load, as shown in Figure 6.
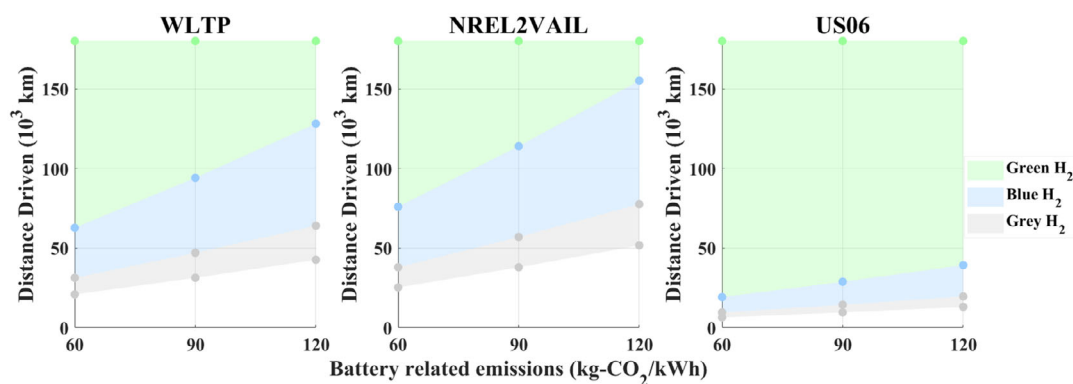
Therefore, the values obtained for the doubled-size battery using the load-based control were used to analyze if the reduced fuel consumption is justified by the extra carbon emissions caused by the battery's increased capacity. Note that the higher the battery restraint losses, as shown in Figure 5, the higher the energy savings, a bigger battery can provide. In an aggressive drive cycle, such as the US06 drive cycle, where there is high braking energy in the deceleration points, it is more favorable to have a bigger battery due to the high battery restrain losses. As shown in Figure 5, for the US06, there is a higher fuel consumption reduction when there is increase in the battery size, that is, about three times higher reduction when doubling the size compared to the other drive cycles. In that case, even the triple-sized battery significantly reduces the fuel consumption, as illustrated in Figure 4. However, since it does compensate for the other drive cycles, the double-sized battery was investigated regarding the environmental compensation. The distance a vehicle should travel to compensate for extra emissions added by the double-sized battery strongly depends on the drive cycle and the source of hydrogen used (green, blue, or gray), as shown in **Figure 7**. Since green hydrogen has low carbon emissions associated with its production, the fuel consumption reduction provided by the addition of a bigger battery is less justified in terms of carbon emissions. Thus, even in the worst case of green hydrogen production emissions and low battery-related emissions, the vehicle should drive about 1/3 of its lifetime, that is, 60 000 km considering a 180 000 km lifetime, to start to compensate for the extra emissions added by the battery. Unless the vehicle is mostly speed-aggressive driving such as in the US06, in that case, much fewer kilometers are already enough, that is, minimum of about 20 000 km for green hydrogen. Thus, as hydrogen production shifts to more sustainable sources, the need for larger batteries becomes less justified for reducing carbon emissions.

For future investigations, considering the trade-off with the cost of bigger batteries should add value to the analysis of increasing the battery capacity. Furthermore, with the advancement of the technologies involved some of the parameters considered in this work, such as manufacturing carbon emissions, might become outdated and in a need of re-evaluation. It can also be pointed out that despite the lower carbon emissions related to green hydrogen, implications such as land use, water

Figure 6. Battery SOC (%) variation in the FCV for the NREL2VAIL drive cycle, while using the control strategies: SOC-based, based on the battery SOC, and load-based, based on the load required from the drive cycle.

Figure 7. Distance driven by the FCV to compensate for the extra emissions provided by the extra weight of a double-sized battery compared to the one-sized battery considering the hydrogen fuel source and the battery manufacturing-related emissions.

consumption, and other lifecycle impacts might also play a role concerning sustainability. Other extreme driving conditions, such as intense cold weather, which was recently pointed out as beneficial to FCV efficiency due to the onboard heating usage,[31] could also bring more understanding to the trade-off between FCV battery sizing and carbon emissions. Concerning the scope of this work, the main outcomes are next summarized.

4. Conclusion

In this work, the impact of increasing the battery size of a FCV was investigated regarding its trade-off between efficiency and sustainability. The main conclusions of this work are: 1) Double-sized batteries (3.2 kWh) compared to the battery size of a commercial FCV could considerably reduce hydrogen consumption. In the control strategy selected, bigger battery sizes would bring fuel savings to the vehicle to compensate for the battery's extra weight just for the aggressive-speed drive cycle. Generalizing these results, the battery size should have enough capacity/pulse charging to take the regenerative braking of the lowest deceleration points. Thus, aggressive-driven profiles are the ones that get most benefit from the battery's increased size. 2) To compensate for the extra carbon emissions added from the double-sized battery, the source of hydrogen used as a fuel and the drive cycle (green, blue, or gray) strongly affects a distance the car should travel. For instance, speed-aggressive drive cycles using gray hydrogen can compensate for the extra carbon emission added by the bigger battery in less than 15 000 km driven. On the other hand, in less-aggressive drive cycles, such as the WLTP, at least 60 000 km should be traveled when fueled by green hydrogen to compensate for the extra carbon emissions provided by the bigger battery.

Conflict of Interest

The authors declare no conflict of interest.

Data Availability Statement

The data that support the findings of this study are available from the corresponding author upon reasonable request.

[1] M. Muratori, M. Alexander, D. Arent, M. Bazilian, P. Cazzola, E. M. Dede, J. Farrell, C. Gearhart, D. Greene, A. Jenn, M. Keyser, T. Lipman, S. Narumanchi, A. Pesaran, R. Sioshansi, E. Suomalainen, G. Tal, K. Walkowicz, J. Ward, *Prog. Energy* **2021**, *3*, 22002.
[2] P. G. Pereirinha, M. González, I. Carrilero, D. Anseán, J. Alonso, J. C. Viera, *Transp. Res. Procedia* **2018**, *33*, 235.
[3] E. M. Bibra, E. Connelly, S. Dhir, M. Drtil, P. Henriot, I. Hwang, J. B. Je Marois, S. McBain, L. Paoli, J. Teter, *Global EV Outlook 2022: Securing Supplies for an Electric Future*, International Energy Agency **2022**, p. 221.
[4] W. Zhang, X. Fang, C. Sun, *J. Environ. Manage.* **2023**, *341*, 118019.
[5] Z. P. Cano, D. Banham, S. Ye, A. Hintennach, J. Lu, M. Fowler, Z. Chen, *Nat. Energy* **2018**, *3*, 279.
[6] U. Khan, T. Yamamoto, H. Sato, *Int. J. Hydrogen Energy* **2022**, *47*, 31949.
[7] G. Krishna, *Transp. Res. Interdiscip. Persp.* **2021**, *10*, 100364.
[8] G. Marbán, T. Valdés-Solís, *Int. J. Hydrogen Energy* **2007**, *32*, 1625.
[9] J. O. Abe, A. P. I. Popoola, E. Ajenifuja, O. M. Popoola, *Int. J. Hydrogen Energy* **2019**, *44*, 15072.
[10] X. Liu, K. Reddi, A. Elgowainy, H. Lohse-Busch, M. Wang, N. Rustagi, *Int. J. Hydrogen Energy* **2020**, *45*, 972.
[11] A. Teimouri, K. Z. Kabeh, S. Changizian, P. Ahmadi, M. Mortazavi, *Int. J. Hydrogen Energy* **2022**, *47*, 37990.
[12] K. Durkin, A. Khanafer, P. Liseau, A. Stjernström-Eriksson, A. Svahn, L. Tobiasson, T. S. Andrade, J. Ehnberg, *Energies* **2024**, *17*, 1085.
[13] P. Ahmadi, A. Khoshnevisan, *Int. J. Hydrogen Energy* **2022**, *47*, 26758.
[14] T. Teng, X. Zhang, H. Dong, Q. Xue, *Int. J. Hydrogen Energy* **2020**, *45*, 20293.
[15] X. Zhao, L. Wang, Y. Zhou, B. Pan, R. Wang, L. Wang, X. Yan, *Energy Convers. Manage.* **2022**, *270*, 116179.
[16] H.-A. Trinh, H. V. A. Truong, T. C. Do, M. H. Nguyen, P. V Du, K. K. Ahn, *Energy Rep.* **2022**, *8*, 6035.
[17] H.-B. Yuan, W.-J. Zou, S. Jung, Y.-B. Kim, *Int. J. Hydrogen Energy* **2022**, *47*, 7932.
[18] T. Fletcher, K. Ebrahimi, *Energies* **2020**, *13*, 5889.
[19] Z. Hu, J. Li, L. Xu, Z. Song, C. Fang, M. Ouyang, G. Dou, G. Kou, *Energy Convers. Manage.* **2016**, *129*, 108.
[20] G. H. Patel, J. Havukainen, M. Horttanainen, R. Soukka, M. Tuomaala, *Green Chem.* **2024**, *26*, 992.
[21] M. Sayer, A. Ajanovic, R. Haas, *Int. J. Hydrogen Energy* **2024**, *65*, 626.
[22] T. Gillespie, *Fundamentals of Vehicle Dynamics*, SAE International, Warrendale, PA **2021**.
[23] J. Břoušek, T. Zvolský, in *MATEC Web Conf.*, EDP Sciences, Les Ulis **2018**, Vol. 234, p. 2004.
[24] J. Lindstr, *Development of an Experimental Permanent-Magnet Motor Drive*, Chalmers University of Technology, Gothenburg, Sweden **1999**.
[25] O. Wallmark, *On Control of Permanent-Magnet Synchronous Motors in Hybrid-Electric Vehicle Applications*, Chalmers University of Technology, Gothenburg, Sweden **2004**.
[26] A. Kolli, A. Gaillard, A. De Bernardinis, O. Bethoux, D. Hissel, Z. Khatir, *Energy Convers. Manage.* **2015**, *105*, 716.
[27] L. Wang, H. Li, *IEEE Trans. Ind. Appl.* **2010**, *46*, 1011.
[28] H. Lohse-Busch, K. Stutenberg, M. Duoba, S. Iliev, Technology assessment of a fuel cell vehicle: 2017 Toyota Mirai. Argonne National Lab.(ANL), Argonne, IL (United States) **2018**.
[29] M. J. Lain, E. Kendrick, *J. Power Sources* **2021**, *493*, 229690.
[30] SPEL, Lithium-Ion Batteries Overview n.d. https://www.capacitorsite.com/lithium.html (accessed: July 17 2024).
[31] T. S. Andrade, S. Zhou, Yang J Di, N. Sharma, R. Jervis, T. Thiringer, *Int. J. Hydrogen Energy* **2024**, *92*, 1493.
[32] M. Chordia, A. Nordelöf, L. A.-W. Ellingsen, *Int. J. Life Cycle Assess.* **2021**, *26*, 2024.